

Measurement of the spin and magnetic moment of ^{23}Al

A. Ozawa,¹ K. Matsuta,² T. Nagatomo,³ M. Mihara,² K. Yamada,³ T. Yamaguchi,⁴ T. Ohtsubo,⁵ S. Momota,⁶ T. Izumikawa,⁷ T. Sumikama,³ Y. Nakashima,² H. Fujiwara,² S. Kumashiro,² R. Matsumiya,² M. Ota,⁵ D. Shinojima,⁵ H. Tanaka,⁵ T. Yasuno,¹ S. Nakajima,⁴ T. Suzuki,⁴ K. Yoshida,³ K. Muranaka,⁴ T. Maemura,⁴ A. Chiba,¹ Y. Utsuno,⁸ M. Fukuda,² K. Tanaka,³ I. Tanihata,⁹ Y. Nojiri,⁶ T. Minamisono,^{2,10} J. R. Alonso,¹¹ G. F. Krebs,¹¹ and T. J. M. Symons¹¹

¹*Institute of Physics, University of Tsukuba, Ibaraki 305-8571, Japan*

²*Graduate School of Science, Osaka University, Osaka 560, Japan*

³*RIKEN, Saitama 351-0198, Japan*

⁴*Faculty of Science, Saitama University, Saitama 338-8570, Japan*

⁵*Department of Physics, Niigata University, Niigata 950-218, Japan*

⁶*Kochi Institute of Technology, Kochi 782-8502, Japan*

⁷*Radioisotope Center, Niigata University, Niigata 951-8510, Japan*

⁸*Advanced Science Research Center, Japan Atomic Energy Agency, Ibaraki 319-1106, Japan*

⁹*TRIUMF, Vancouver, British Columbia V6T 2A3, Canada*

¹⁰*Fukui University of Technology, Fukui 910-8505, Japan*

¹¹*Lawrence Berkeley National Laboratory, Berkeley, California 94720, USA*

(Received 20 December 2005; published 1 August 2006)

For the first time, we obtained the g factor for the ground state of ^{23}Al by use of a β -NMR measurement. ^{23}Al has a small proton separation energy and is a potential proton-halo candidate. The obtained g factor, $|g| = 1.557 \pm 0.088$, clearly shows the spin and parity, $J^\pi = 5/2^+$, for ^{23}Al , which is the same as that of its mirror partner, ^{23}Ne . The possible nuclear structure of ^{23}Al is also discussed.

DOI: [10.1103/PhysRevC.74.021301](https://doi.org/10.1103/PhysRevC.74.021301)

PACS number(s): 21.10.Ky, 21.10.Hw, 27.30.+t

Studies of exotic nuclei far from the stability line have attracted much interest during the past two decades since the first observation of the neutron halo in ^{11}Li [1]. Further experiments have confirmed the neutron halo in ^{11}Li , and have also shown the existence of a neutron halo in other neutron-rich nuclei [2]. However, the number of experiments on the proton halo are relatively few compared with those on the neutron halo. Recently, experimental evidence for the proton halo in very proton-rich nuclei has become available: ^8B [3–5], ^{17}Ne [6,7], and $^{26,27,28}\text{P}$ [8]. ^{23}Al is one of the potential candidates for a proton-halo nucleus, because its proton separation energy is quite small (125 keV). Recently, a large reaction cross section of ^{23}Al was measured at the intermediate energy ($\sim 36A$ MeV), although the error was still large [9,10]. The authors of Ref. [9,10] analyzed the data by a Glauber model with simply a core nucleus (^{22}Mg) plus a valence proton (p) configuration. According to their analysis, the density distribution of ^{23}Al should have a halolike long tail. Because the density of a loosely bound s -wave proton can be extended, it is suggested that the spin and parity (J^π) of ^{23}Al might be $1/2^+$. However, the J^π of its mirror partner, ^{23}Ne , is $5/2^+$. Thus, if the ground-state J^π of ^{23}Al is $1/2^+$, the proton halo structure can be anticipated, but the mirror symmetry will be broken between the bound ground states of mirror pairs, which has not been observed for known nuclei so far. Because the magnetic moment of its mirror partner, ^{23}Ne , is known to be -1.077 ± 0.004 [11], the magnetic moment of ^{23}Al allows one to discuss the spin expectation value [12] of the $A = 23$ mirror pair with $T = 3/2$, where T is the isobaric spin. In p -shell nuclei, the ^9C - ^9Li mirror moments ($T = 3/2$) yield an anomalous large spin expectation value, which suggests an

exotic structure of proton-rich ^9C [13]. A similar anomaly may be found in the sd -shell region.

Determining the ground-state J^π of ^{23}Al is also important from a nuclear astrophysical aspect. The $^{22}\text{Mg}(p,\gamma)^{23}\text{Al}$ reaction is relevant to the nucleosynthesis of ^{22}Na in Ne-rich novae [14]. The ^{22}Na yield might be reduced if an escape from the reaction sequence takes place via the $^{22}\text{Mg}(p,\gamma)^{23}\text{Al}$ reaction. In novae, resonant capture through the first excited state contributes dominantly, because the first excited state of ^{23}Al , lying at 405 keV above the proton threshold, locates near the Gamow energy. To calculate the strength of the resonant capture, determining the spin of the first excited state of ^{23}Al is necessary [15]. In the previous works [16,17], $J^\pi = 1/2^+$ is suggested for the first excited state, which implies $J^\pi = 5/2^+$ for the ground state. Thus, if the ground-state J^π is $5/2^+$, the suggestions by the previous works will be supported.

Until now, there has been no direct measurement for J^π of ^{23}Al . The β decay of ^{23}Al to excited states in ^{23}Mg has been investigated [18]. Although the β -decay branching ratio to the ground state ($J^\pi = 3/2^+$) of ^{23}Mg has not been measured, the strength of β -decay branches to the excited states in ^{23}Mg strongly suggested $J^\pi = 5/2^+$ for the ground state of ^{23}Al . The magnetic moment allows us to determine the spin and parity directly, because the magnetic moment is very different for the different spin [19]. Therefore, we measured the magnetic moment of ^{23}Al .

The ^{23}Al nuclei were produced through the projectile-fragmentation process in the collision of ^{28}Si on a ^9Be target, as the RI beam. The primary beam of ^{28}Si was accelerated up to 135A MeV by the RIKEN ring cyclotron. The Be target thickness was 4.0 mm. Only the fragments ejected at angles of

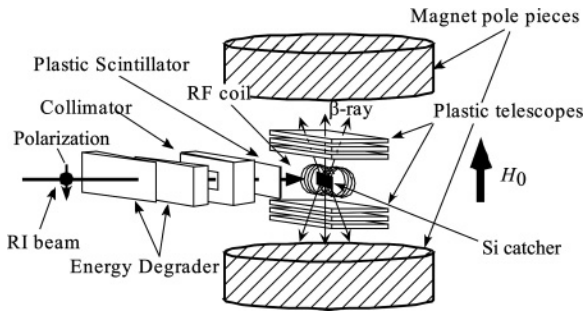


FIG. 1. Experimental setup for the magnetic moment measurements of ^{23}Al .

$1.0^\circ \pm 0.6^\circ$ were separated by the fragment separator, RIPS. In the separator, the momentum of the fragments was analyzed, and only the fragments with a momentum $2.0 \pm 0.5\%$ larger than the central momentum were selected. The projectile fragments were polarized with this selection of the reaction angle and the momentum [20]. The major contaminants in the RI beam were isotones of ^{23}Al : ^{22}Mg , ^{21}Na , and so on. To sweep the isotones of ^{23}Al , an RF deflector [21] was installed at the achromatic focus, F2, of the RIPS. The S/N ratio in the RI beam was improved from 0.024 to 0.17 by use of an RF deflector.

Experimental setup for the magnetic moment measurements is shown in Fig. 1. The selected fragments were slowed down by an energy degrader and were implanted in a Si catcher of 0.6 mm in thickness placed in a strong magnetic field, H_0 , of 3.0005 ± 0.0006 kOe to maintain the polarization. Count rate of the RI beam was monitored by the plastic scintillator located after the energy degrader. Typical total count rate of the RI beam during the measurements was ~ 4000 cps. β rays emitted from the stopped ^{23}Al (the maximum β -ray energy, $Q_\beta = 12218$ keV) were detected during the beam-off time after beam bombardment by use of two sets of plastic-scintillation-counter telescopes placed above and below the catcher relative to the reaction plane. 1.0-mm-thick Cu absorber was placed in between the first and second scintillators of the each telescopes to absorb low-energy β rays emitted from the contaminants of the RI beam. For example, β rays with $Q_\beta \sim 4$ MeV can be absorbed. The β rays from ^{22}Mg ($Q_\beta = 4786$ keV) and ^{23}Mg ($Q_\beta = 4056$ keV), which is the daughter nucleus of ^{23}Al , were absorbed. The S/N ratio in the β -ray counts was improved to 1.91 ± 0.17 by use of the Cu absorbers. Thus, we obtained a clean decay curve, where a beam-on production time was 0.5 sec followed by a beam-off time of 5.0 sec, as shown in Fig. 2. The typical count rates of the β rays in the magnetic moment measurements, where a beam-on production time was 0.5 sec followed by a beam-off time of 1.0 sec, were ~ 6 cps in total. The polarization of the ^{23}Al was detected by the β -ray asymmetry in the counter system. An RF magnetic field, H_1 , of about 13 Oe was applied to induce transitions between the magnetic sublevels, resulting in an inversion of the initial polarization. The adiabatic fast passage technique in NMR [22] was employed for inverting the spin polarization under the on-resonance condition.

We performed two measurements with different setups. In the first measurement, the space from the final energy degrader

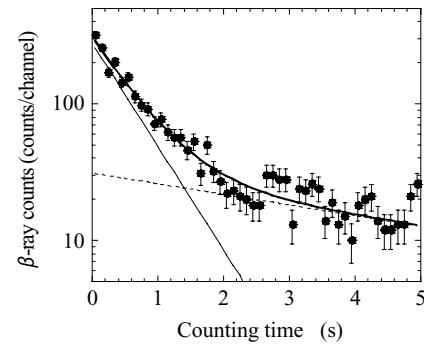


FIG. 2. Typical β -ray time spectrum. Experimental data are shown by closed circles. The thick solid, thin solid, and broken lines show the total, ^{23}Al , and ^{22}Mg components fitted by exponential functions with known half-lives, respectively.

to the entrance of the catcher chamber was filled with He gas. In the second measurement, the whole region from the final energy degrader to the catcher was in a vacuum so as to completely remove any polarization destruction by gas collisions before the catcher. Preliminary results of the first measurement are shown in Ref. [23].

A NMR spectrum for wide frequency modulation (FM) of ± 500 kHz is shown in the upper part of Fig. 3. The data were averaged by the first and the second measurements. We found a resonance at around 3600 kHz. To determine the resonance more precisely, we performed measurements with a narrow FM of ± 200 kHz. The obtained NMR spectra are shown in the lower part of Fig. 3. For fitting the NMR spectrum, we took into account the width of the FM and the strength of the magnetic fields. The fitting function, $S(\omega)$, is given by

$$S(\omega) = \frac{1 - \cos \alpha(\omega) \cdot \cos \beta(\omega)}{2} AP, \quad (1)$$

where A is the β -decay asymmetry parameter and P is the spin polarization. The $\alpha(\omega)$ and $\beta(\omega)$ are defined by the direction

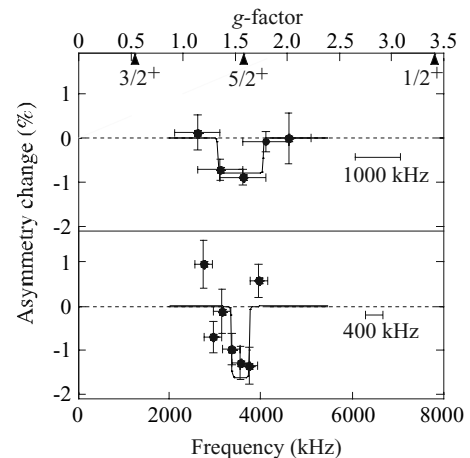


FIG. 3. Observed β NMR spectra. The upper (lower) part is the spectrum with ± 500 kHz (± 200 kHz) frequency modulation, respectively. The solid lines show the results by the fitting procedure. Predictions of the g factor by our shell-model calculations are shown by the arrows.

of the nuclear spin at the start of FM and the end of FM to the H_0 , as given by

$$\cot \alpha(\omega) = \frac{\omega_0 - (\omega - \omega_{\text{FM}})}{\omega_1} \quad (2)$$

and

$$\cot \beta(\omega) = \frac{\omega_0 - (\omega + \omega_{\text{FM}})}{\omega_1},$$

where $\omega_0 = g\mu_N H_0/\hbar$ is the Larmor frequency, $\omega_1 = g\mu_N H_1/\hbar$, and ω_{FM} is the half-width of the FM. The fitting results are shown by the lines in Fig. 3. The resonance frequency was determined to be 3558.8 ± 15.8 (statistical) ± 200 (systematical) kHz. It is noted that the statistical error was determined by the average of the data with a wide and narrow FM, and the systematical errors was given by the width of a narrow FM. By using the resonance frequency, the g factor was determined to be $|g| = 1.556 \pm 0.088$, where any statistical and systematical errors were simply weighted. We took into account a small diamagnetic correction ($8.3 \pm 0.5 \times 10^{-4}$) in the Si stopper [24]. Thus, the final g factor was 1.557 ± 0.088 .

We performed shell-model calculations to assign the spin and parity of ^{23}Al . We used the OXBASH code with the USD interaction for the shell-model calculations [25]. At first, we calculated the magnetic moment of ^{23}Ne , which is a mirror pair of ^{23}Al , to check the validity of the calculation. The calculated magnetic moment for ^{23}Ne is $g = -1.129$, which is consistent with the known value of $g = -1.077 \pm 0.004$. For ^{23}Al , our shell-model calculations show $g = +3.410$ for $J^\pi = 1/2^+$, $g = +0.538$ for $J^\pi = 3/2^+$, and $g = +1.575$ for $J^\pi = 5/2^+$, respectively. Here, the nucleon g factors in free space were used for the calculations. The calculated values are shown by arrows in Fig. 3. The calculated values are not sensitive to the choices of the nucleon g factors. If we use the effective nucleon g factors [25], $g = +1.591$ for $J^\pi = 5/2^+$. It is also noted that, even if we use different types of interactions or different single-particle energies, where $J^\pi = 1/2^+$ or $J^\pi = 3/2^+$ becomes the ground state, each g factor changes by only ~ 0.3 . The present experimental g factor is well reproduced by the shell-model value for the ground state J^π of $5/2^+$, as shown in Fig. 3. The shell-model values for $J^\pi = 1/2^+$ and $3/2^+$ strongly deviate from the present experimental value. This clearly shows that the ground-state J^π of ^{23}Al is $5/2^+$. Thus, the magnetic moment, $\mu(=gJ)$, of ^{23}Al was determined to be $|\mu| = 3.89 \pm 0.22 \mu_N$. The obtained results of the magnetic moment of ^{23}Al and its energy levels with those of neighbors are shown in Fig. 4.

The ground-state J^π of ^{23}Al can give a strong restriction to the possible nuclear structure of the nucleus. Because the proton separation energy of ^{23}Al is fairly small, a core nucleus plus a valence proton ($^{22}\text{Mg}+p$) structure can be anticipated. If we assume the $^{22}\text{Mg}+p$ structure, $J^\pi = 5/2^+$ allows three different configurations: (i) the ground state of ^{22}Mg ($J^\pi = 0^+$) couples to the d -wave valence proton, (ii) the first excited state of ^{22}Mg ($E_x = 1.25$ MeV, $J^\pi = 2^+$) couples to the s -wave valence proton, and (iii) the first excited state of ^{22}Mg couples to the d -wave valence proton. Our shell-model calculations show that the configuration of case (i) is 71%, that of case

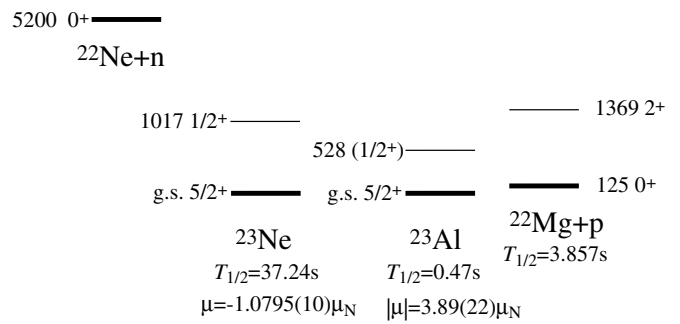


FIG. 4. Level schemes (in keV) with the related information of $^{22}\text{Ne}+n$, ^{23}Ne , ^{23}Al , and $^{22}\text{Mg}+p$. Only low-lying excited states are shown.

(ii) is only 0.2%, and that of case (iii) is 23%. It is noted that, in the mirror partner ^{23}Ne , the d -wave valence neutron is dominant in the ground state, which was shown by the $^{22}\text{Ne}(d, p)^{23}\text{Ne}$ reactions [26]. Thus, the configuration with the d -wave valence proton is the most probable for ^{23}Al .

It is noted how the authors concluded the proton halo structure for ^{23}Al . They measured reaction cross sections of ^{23}Al and ^{22}Mg at $\sim 36A$ MeV and found a much larger reaction cross section for ^{23}Al than for ^{22}Mg . To reproduce the enhancement by the simple $^{22}\text{Mg}+p$ configuration based on the Glauber model, the halolike tail is needed for ^{23}Al . Loosely bound s -wave protons can extend its density so much because of no centrifugal barrier ($l = 0$) [27]. Thus the authors of Refs. [9,10] concluded $J^\pi = 1/2^+$ for ^{23}Al . However, if the J^π of ^{23}Al is $5/2^+$, the d -wave proton is dominant, as discussed above. Thus, the large reaction cross section of ^{23}Al compared to that of ^{22}Mg cannot be explained by the simple $^{22}\text{Mg}+p$ configuration based on the Glauber model. A similar puzzle is also observed in ^{19}C and ^{23}O . In both nuclei, large interaction cross sections cannot be reproduced by the simple core+neutron configuration, even for the pure s -wave valence neutron [28,29]. One solution may be to introduce a core modification [30]. Although the core+valence nucleon structure is fulfilled, the density of the core nucleus is much larger than that in the free space. Thus, the large reaction-interaction cross sections of these nuclei are because of the large density of the core.

The spin expectation value can be determined from the present result combined with the magnetic moment of the mirror partner, ^{23}Ne . For the calculation, the sign of the magnetic moment of ^{23}Al was assumed to be positive, which is predicted by our shell-model calculation. Thus, the spin expectation value was determined to be $+0.8 \pm 0.6$. The present error is still large for further discussion about detailed configuration mixing of the nucleus. Experimental results of magnetic moments of the mirror pair with $T = 3/2$ nearby $A = 23$ are noted. Very recently, magnetic moments of ^{17}Ne [11] and ^{35}K [31] have been measured. Thus, the mirror pair with $T = 3/2$ for $A = 17$ and $A = 35$ can be discussed. For both systems, no anomalous spin expectation values have not been observed. For $A = 21$ and $A = 25$, magnetic moments of neutron rich nuclei (^{21}F and ^{25}Na) are experimentally known [32]. Thus, if we measure the magnetic moments of

^{21}Mg ($J^\pi = 5/2^+$) and ^{25}Si ($J^\pi = 5/2^+$), the spin expectation value can be extracted.

For ^{23}Al , one unbound excited state with $E_x=528$ keV is known, as shown in Fig. 4. Our shell-model calculation shows that J^π of the first excited state is $1/2^+$ if the ground state of ^{23}Al is $J^\pi = 5/2^+$. These assignments are important to estimate the strength of the resonant capture in the $^{22}\text{Mg}(p, \gamma)^{23}\text{Al}$ reaction.

In summary, the g factor of the ground state of ^{23}Al , which is a potential proton-halo candidate, has been measured for the first time. The obtained $|g| = 1.557 \pm 0.088$ clearly shows the spin and parity $J^\pi = 5/2^+$ for ^{23}Al , which was strongly suggested by the previous β -decay measurement [18]. Thus, the mirror symmetry is fulfilled in the ground states between ^{23}Al and ^{23}Ne . Determining the spin and parity provides a strong restriction to the possible nuclear structure of ^{23}Al . If we assume a simple $^{22}\text{Mg}+p$ structure for ^{23}Al , a configuration, including the d -wave valence proton, is most probable for ^{23}Al . However, previously observed large reaction cross section of the nucleus at the intermediate energy ($\sim 36A$ MeV) cannot be

reproduced well. Experimentally, more reliable and accurate measurements of the reaction cross sections are urged with different energies. Energy dependences of the reaction cross sections can describe effective matter densities of ^{23}Al in detail [4]. Concerning a possible proton halo structure of ^{23}Al , measurements of the momentum distribution of fragments from ^{23}Al and the quadrupole moment of ^{23}Al will give more information. The present result on the ground state spin and parity may remove any uncertainty in estimating the strength of the resonant capture cross section of $^{22}\text{Mg}(p, \gamma)^{23}\text{Al}$. Previously, the ground state of $J^\pi = 5/2^+$ and the first excited state of $J^\pi = 1/2^+$ in ^{23}Al were assumed [15]. The present measurements show that the above spin assignments are proper.

The present work was performed at the RIKEN Ring Cyclotron. The authors are grateful to the staff of RIKEN for their technical support. Support was also given by a grant-in-aid for Scientific Research from the Ministry of Education, Culture and Science, Japan.

-
- [1] I. Tanihata *et al.*, Phys. Rev. Lett. **55**, 2676 (1985).
 [2] A. S. Jensen and M. V. Zhukov, Nucl. Phys. **A693**, 411 (2001).
 [3] T. Minamisono *et al.*, Phys. Rev. Lett. **69**, 2058 (1992).
 [4] M. Fukuda *et al.*, Nucl. Phys. **A656**, 209 (1999).
 [5] D. Cortina-Gil *et al.*, Nucl. Phys. **A720**, 3 (2003).
 [6] R. Kanungo *et al.*, Phys. Lett. **B571**, 21 (2003).
 [7] K. Tanaka *et al.*, Nucl. Phys. **A746**, 532c (2004).
 [8] A. Navin *et al.*, Phys. Rev. Lett. **81**, 5089 (1998).
 [9] X. Z. Cai *et al.*, Phys. Rev. C **65**, 024610 (2002).
 [10] H. Y. Zhang *et al.*, Nucl. Phys. **A707**, 303 (2002).
 [11] W. Geithner *et al.*, Phys. Rev. C **71**, 064319 (2005).
 [12] K. Asahi and K. Matsuta, Nucl. Phys. **A693**, 63 (2001).
 [13] K. Matsuta *et al.*, Nucl. Phys. **A588**, 153c (1995).
 [14] C. E. Rolfs and W. S. Rodney, *Cauldrons in the Cosmos* (University of Chicago press, Chicago, 1988), p. 376.
 [15] T. Gomi *et al.*, Nucl. Phys. **A734**, E77 (2004).
 [16] M. Wiescher *et al.*, Nucl. Phys. **A484**, 90 (1988).
 [17] J. A. Caggiano *et al.*, Phys. Rev. C **64**, 025802 (2001).
 [18] K. Perajarvi *et al.*, Phys. Lett. **B492**, 1 (2000).
 [19] H. Ogawa *et al.*, Eur. Phys. J. A **13**, 81 (2002).
 [20] H. Okuno *et al.*, Phys. Lett. **B335**, 29 (1994).
 [21] K. Yamada *et al.*, Nucl. Phys. **A746**, 156c (2004).
 [22] A. Abragam, *Principles of Nuclear Magnetism* (Clarendon Press, Oxford, 1986), p. 66.
 [23] K. Matsuta *et al.*, Hyperfine Interactions **159**, 257 (2004).
 [24] F. D. Feiock and W. R. Johnson, Phys. Rev. **187**, 39 (1969).
 [25] B. A. Brown and B. H. Wildenthal, Annu. Rev. Nucl. Part. Sci. **38**, 29 (1988).
 [26] A. J. Howard *et al.*, Nucl. Phys. **A152**, 317 (1970).
 [27] M. M. Obuti *et al.*, Nucl. Phys. **A609**, 74 (1996).
 [28] R. Kanungo *et al.*, Nucl. Phys. **A677**, 171 (2000).
 [29] A. Ozawa *et al.*, Nucl. Phys. **A691**, 599 (2001).
 [30] R. Kanungo *et al.*, Phys. Rev. Lett. **88**, 142502 (2002).
 [31] T. J. Mertzimekis, P. F. Mantica, A. D. Davies, S. N. Liddick, and B. E. Tomlin, Phys. Rev. C **73**, 024318 (2006).
 [32] N. J. Stone, At. Data Nucl. Data Tables **90**, 75 (2005).